Interaction Notes

Note 436

21 February 1984

# FINITELY CONDUCTING, INFINITELY LONG, CYLINDRICAL WIRE IN THE PRESENCE OF A PLANE WAVE (EMP)*

H. P. Neff, Jr.
University of Tennessee
Knoxville, Tennessee

D. A. Reed
University of Tennessee
Knoxville, Tennessee

## Abstract

The time-domain current induced in an infinitely long, finitely conducting wire in the presence of a plane electromagnetic wave with its magnetic field perpendicular to the wire axis is determined by first finding the frequency-domain (phasor) solution. This is accomplished by using both a magnetic vector potential and an electric vector potential, and then treating the problem as a boundary-value problem. The time-domain current is found by performing the inverse Fourier transform numerically. Results indicate that the early time behavior is essentially that of a lossless wire, and the major effect is that the current dies out for large time much faster with loss than without loss.

*The research reported in this Note was sponsored by the Division of Electric Energy Systems of the Department of Energy, and was performed under Subcontract No. 7685 PAS38 with Martin Marietta Corp. for Oak Ridge National Laboratory.

## 1. INTRODUCTION

When an infinitely-long, finitely-conducting, and circular-cylindrical, wire is exposed to a plane wave in (otherwise) free space, it is a relatively straightforward, but perhaps lengthy, matter to analytically determine the quantities of interest, such as induced current. This can be accomplished with potential theory, treating the problem as a boundary-value problem. When the desired quantity has been found, its time-domain form can be found by means of the inverse Fourier transform (performed numerically), or by finding (numerically) its unit-impulse response, and then using convolution (numerically). Numerical integration is required because of the non-standard forms that occur.

## II. FORMULATION OF THE PROBLEM

It is assumed that the electric field vector, the Poynting vector, and the wire axis lie in the same plane. The geometry is shown in Figure 1. The induced axial current for the perfect conductor case ($\sigma \to \infty$) is well known,[1,2] and is given by

$$I_z = \frac{4E_0}{\omega\mu_0 \sin\theta} e^{-jk_z z} \frac{1}{H_0^{(2)}(k_\varrho a)} \tag{1}$$

where

$E_0$ = peak value of the incident electric field of the (phasor) plane wave.

$\mu_0 = 4\pi \times 10^{-7}$ = permeability of air.

$k_z = k \cos\theta = \omega\sqrt{\mu_0\varepsilon_0} \cos\theta.$

$k_\varrho = k \sin\theta = \omega\sqrt{\mu_0\varepsilon_0} \sin\theta.$

$\varepsilon_0 = 10^{-9}/36\pi$ = permittivity of air.

$H_0^{(2)}(k_\varrho a)$ = Hankel function, second kind, order zero

$\theta$ = angle between the wire axis and the Poynting vector of the incident plane wave.

$|I_z/E_0|$ in dB* and $\underline{|I_z/E_0}$ in degrees versus $\omega$ (logarithmic scale) are shown (dotted) in Figure 2 for equation (1) with $z = 0$, $a = 0.00715$ m and $\theta = 54°$ in Figure 2 for the purpose of comparison with the finite loss case.

The task here is to produce a similar result for the case where the wire is finitely conducting ($\sigma$ = conductivity). Figure 1 applies to this problem as well. The incident field is

$$E_x^{inc} = -E_0 \cos\theta\, e^{-jk(x\sin\theta + z\cos\theta)} \tag{2}$$

$$E_z^{inc} = +E_0 \sin\theta\, e^{-jk(x\sin\theta + z\cos\theta)} \tag{3}$$

---

*$20 \log_{10}|I_z/E_0|$

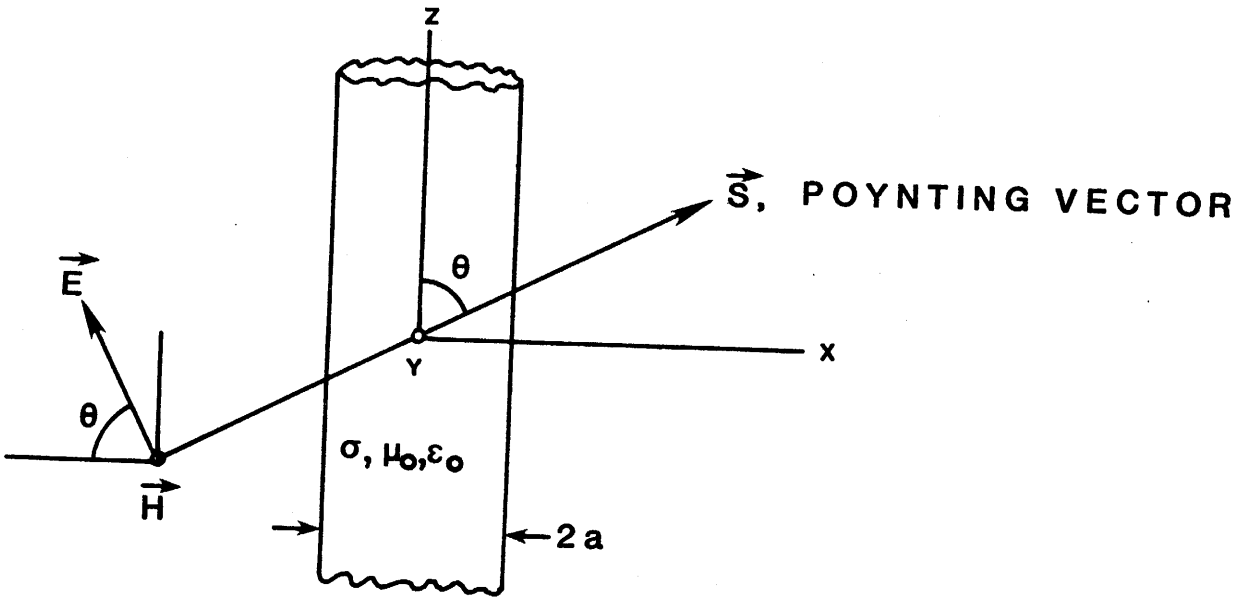


Figure 1. Geometry of the problem.

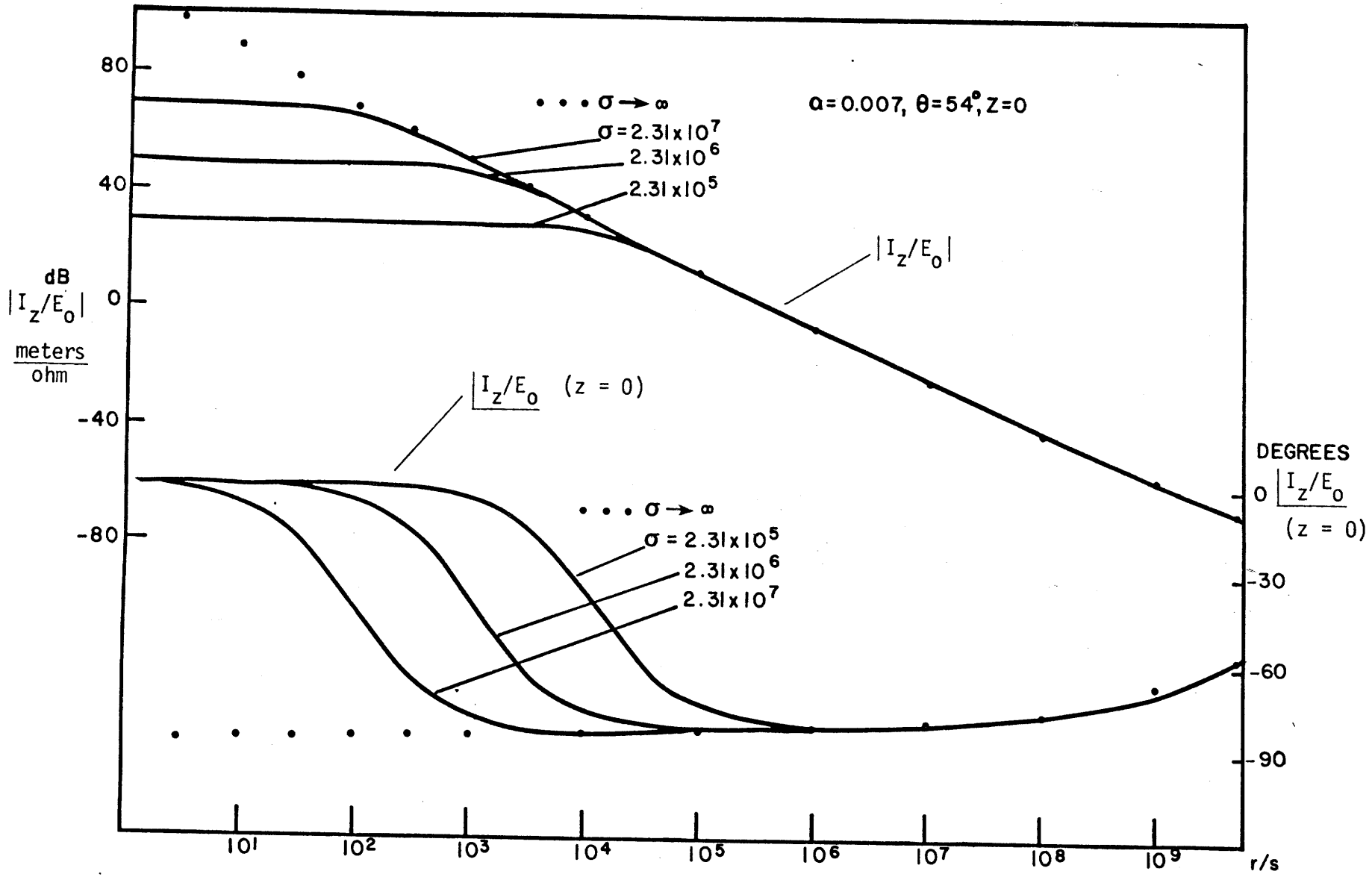


Figure 2. $I_z(\omega)$ versus $\omega$ (magnitude in dB and angle in degrees) for various wire conductivities; $\theta = 54°$, $a = 0.00715$, $z = 0$, $E_0 = 1$.

$$H_y^{inc} = -\frac{E_o}{\eta_o} e^{-jk(x\sin\theta + z\cos\theta)} \tag{4}$$

where $\eta_o = \sqrt{\mu_o/\varepsilon_o}$. This incident field is derivable from a z-directed magnetic vector potential:

$$A_z^{inc} = \frac{jE_o}{\omega\sin\theta} e^{-jk(x\sin\theta + z\cos\theta)} \tag{5}$$

$$A_z^{inc} = \frac{jE_o}{\omega\sin\theta} e^{-jk(\varrho\cos\phi\sin\theta + z\cos\theta)}$$

$$A_z^{inc} = \frac{jE_o}{\omega\sin\theta} e^{-jk_z z} e^{-jk_\varrho \varrho\cos\phi} \tag{6}$$

The last exponential in (6) can be expressed in terms of ordinary Bessel functions by way of the Fourier series so that

$$A_z^{inc} = \frac{jE_o}{\omega\sin\theta} e^{-jk_z z} \sum_{n=-\infty}^{\infty} j^{-n} J_n(k_\varrho \varrho) e^{jn\phi} \tag{7}$$

This vector potential fits the general solution to the wave equation:

$$e^{-jk''_z z} \sum_{n=-\infty}^{\infty} g_n B_n(k''_\varrho \varrho) e^{jn\phi} \tag{8}$$

where $k^2 = \omega^2\mu\varepsilon = (k''_z)^2 + (k''_\varrho)^2$, and $B_n$ is any Bessel function or linear combination of Bessel functions.

The total field consists of the incident field just described plus the scattered field and the internal (to the wire) field. The internal field must be finite on the z axis, so $B_n$ must be $J_n$. If $E_\varrho$ and (or) $E_\phi$, as well as $E_z$, exist

within the cylinder, then $H_z$ must exist within the cylinder since there will be azimuthal and radial (respectively) components of current that must be encircled by a magnetic field such that $H_z \equiv 0$. Thus, an electric vector potential $F_z$ is also required for the internal field. The scattered field then also requires both $A_z$ and $F_z$ in order that boundary conditions can be satisfied at the wire surface ( $\varrho = a$). Thus, for the incident, scattered, and internal fields we must have the forms

$$A_z^{inc} = e^{-jk_z z} \sum_{n=-\infty}^{\infty} f_n J_n(k_\varrho \varrho) e^{jn\phi}, \; F_z^{inc} \equiv 0 \tag{9}$$

$$A_z^{sc} = e^{-jk_z z} \sum_{n=-\infty}^{\infty} a_n H_n^{(2)}(k_\varrho \varrho) e^{jn\phi}, \; F_z^{sc} = e^{-jk_z z} \sum_{n=-\infty}^{\infty} b_n H_n^{(2)}(k_\varrho \varrho) e^{jn\phi} \tag{10}$$

$$A_z^{int} = e^{-jk_z z} \sum_{n=-\infty}^{\infty} c_n J_n^{(2)}(k'_\varrho \varrho) e^{jn\phi}, \; F_z^{int} = e^{-jk_z z} \sum_{n=-\infty}^{\infty} d_n J_n(k'_\varrho \varrho) e^{jn\phi} \tag{11}$$

in order to satisfy conditions at $\varrho = 0$, $\varrho = a$, and $\varrho \to \infty$.

In terms of $A_z$ and $F_z$ the field is

$$E_\varrho = \frac{1}{j\omega\mu\varepsilon} \frac{\partial^2 A_z}{\partial \varrho \partial z} - \frac{1}{\varrho} \frac{\partial F_z}{\partial \phi}, \; H_\varrho = \frac{1}{\mu\varrho} \frac{\partial A_z}{\partial \phi} + \frac{1}{j\omega\mu} \frac{\partial^2 F_z}{\partial \varrho \partial z} \tag{12}$$

$$E_\phi = \frac{1}{j\omega\mu\varepsilon\varrho} \frac{\partial^2 A_z}{\partial \phi \partial z} + \frac{\partial F_z}{\partial \varrho}, \; H_\phi = -\frac{1}{\mu} \frac{\partial A_z}{\partial \varrho} + \frac{1}{j\omega\mu\varrho} \frac{\partial^2 F_z}{\partial \phi \partial z} \tag{13}$$

$$E_z = \frac{1}{j\omega\mu\varepsilon} (k^2 - k_z^2) A_z, \; H_z = \frac{1}{j\omega\mu} (k^2 - k_z^2) F_z \tag{14}$$

where

$$\left.\begin{aligned} \mu &= \mu_o \\ \varepsilon &= \varepsilon_o \end{aligned}\right\}$$

$$k = \omega\sqrt{\mu_o\varepsilon_o}$$

$$k_z = \omega\sqrt{\mu_o\varepsilon_o}\cos\theta$$

$$k_\varrho = \omega\sqrt{\mu_o\varepsilon_o}\sin\theta$$

} incident and scattered fields (15)

$$\mu = \mu_o$$

$$\varepsilon = \varepsilon' = \varepsilon_o(1 + \sigma/j\omega\varepsilon_o)$$

$$k = k' = \omega\sqrt{\mu_o\varepsilon'}$$

$$k_z = \omega\sqrt{\mu_o\varepsilon_o}\cos\theta$$

$$k'_\varrho = \sqrt{(k')^2 - k_z^2} = \omega\sqrt{\mu_o\varepsilon_o}\sqrt{\varepsilon'/\varepsilon_o - \cos^2\theta}$$

} internal field (16)

The four unknowns in the set (12), (13), and (14) are $a_n$, $b_n$, $c_n$ and $d_n$ when (9), (10), and (11) are used. The four boundary conditions are:

$$E_z^{inc}|_{\varrho=a} + E_z^{sc}|_{\varrho=a} = E_z^{int}|_{\varrho=a} \quad (17)$$

$$E_\phi^{inc}|_{\varrho=a} + E_\phi^{sc}|_{\varrho=a} = E_\phi^{int}|_{\varrho=a} \quad (18)$$

$$H_z^{sc}|_{\varrho=a} = H_z^{int}|_{\varrho=a} \quad (19)$$

$$H_\phi^{inc}|_{\varrho=a} + H_\phi^{sc}|_{\varrho=a} = H_\phi^{int}|_{\varrho=a} \quad (20)$$

Thus, it is a straightforward, but lengthy, matter to solve for the unknown coefficients.

The total axial current is given by

$$I_{zt} = \int_0^{2\pi} H_\phi^{int}\big|_{\varrho = a} a\, d\phi = 2\pi a\, H_\phi^{int}\big|_{\varrho = a,\, n=0} \tag{21}$$

This is the sum of conduction and displacement currents

$$I_{zt} = \frac{2\pi a}{\mu_o} k'_\varrho\, e^{-jk_z z}\, c_o J_1(k'_\varrho a)$$

or, when $c_o$ is substituted,

$$I_{zt} = \frac{4E_o}{\omega \mu_o \sin\theta} e^{-jk_z z} \frac{1}{H_o^{(2)}(k_\varrho a) - \frac{k'_\varrho \varepsilon_o}{k_\varrho \varepsilon'} \frac{J_o(k'_\varrho a)}{J_1(k'_\varrho a)} H_1^{(2)}(k_\varrho a)} \tag{22}$$

Maxwell's second equation (Ampere's generalized law) shows that the ratio of the conduction current to the total current (conduction plus displacement) is given by

$$\frac{I_{zc}}{I_{zc} + I_{zd}} = \frac{\sigma}{j\omega\varepsilon'} = \frac{\sigma}{\sigma + j\omega\varepsilon_o} = \frac{1}{1 + j\omega\varepsilon_o/\sigma} \tag{23}$$

Therefore, the axial conduction current is

$$I_{zc} = \frac{4E_o}{\omega \mu_o \sin\theta} e^{-jk_z z} \frac{1}{H_o^{(2)}(k_\varrho a) - \frac{k'_\varrho \varepsilon_o}{k_\varrho \varepsilon'} \frac{J_o(k'_\varrho a)}{J_1(k'_\varrho a)} H_1^{(2)}(k_\varrho a)} \frac{1}{1 + j\omega\varepsilon_o/\sigma} \tag{24}$$

Several special cases need to be investigated.

Equation (24 should agree with (1) for $\sigma \to \infty$ or [from (16)] $\varepsilon' \to \infty$ and $k'_\varrho \to \infty$. The Bessel functions are oscillatory for large k', but

$$\frac{k'_\varrho \varepsilon_o}{k_\varrho \varepsilon'} = \frac{1}{\sin\theta} \sqrt{\varepsilon_0/\varepsilon' - (\varepsilon_0/\varepsilon')^2 \cos^2\theta} \qquad \to 0$$

$$\varepsilon' \to \infty$$

and the second terms in both denominators in (24) disappear for $\sigma \to \infty$. Equation (24) is then identical to (1) for the perfect conductor case.

For very low frequency $\omega \to 0$, or [from (16)] $k'_\varrho \to 0, k_z \to 0$, and

$$H_o^{(2)}(k_\varrho a) \to 1 - j\frac{2}{\pi}\ln(\gamma\, k_\varrho a/2),\ \omega << \frac{1}{a\sqrt{\mu_o\varepsilon_o}\sin\theta},\ \gamma = 1.781$$

$$H_1^{(2)}(k_\varrho a) \to j\frac{2}{\pi}\frac{1}{k_\varrho a} \qquad ,\ \omega << \frac{1}{a\sqrt{\mu_o\varepsilon_o}\sin\theta}$$

$$\frac{k'_\varrho \varepsilon_o}{k_\varrho \varepsilon'} \to \frac{1}{\sin\theta\sqrt{\sigma/\omega\varepsilon_o}}\, e^{j\pi/4} \qquad ,\ \omega << \sigma/\varepsilon_o$$

$$\frac{J_o(k'_\varrho a)}{J_1(k'_\varrho a)} \to \frac{2}{a\sqrt{\omega\mu_o\sigma}}\, e^{j\pi/4} \qquad ,\ \omega << \frac{1}{a^2\mu_o\sigma}$$

The last inequality in the preceding set is the dominant one for most cases of practical interest. Thus

$$I_{zc} \to \frac{4E_o}{\omega\mu_o\sin\theta - j\frac{2}{\pi}\omega\mu_o\sin\theta\ln(\gamma k_\varrho a/2) + \frac{4}{\pi a^2\sigma\sin\theta}}$$

$\omega \to 0$

and

$$I_{zc}(0) = \pi a^2\sigma\sin\theta\, E_o(0) \qquad (\omega = 0) \tag{25}$$

This dc current is as expected. On the other hand, if the Hankel functions in (24) are retained, and the low frequency case reconsidered with

$$\frac{k'_\varrho \varepsilon_o}{k_\varrho \varepsilon'}\frac{J_o(k'_\varrho a)}{J_1(k'_\varrho a)} \approx j\frac{2}{\sigma a\sin\theta\sqrt{\mu_o/\varepsilon_o}}$$

$$= j\frac{1}{60\pi\sigma a\sin\theta},\ \omega << \frac{1}{a^2\mu_o\sigma}$$

as above, then (24) becomes

$$I_{zc} \approx \frac{4E_o}{\omega\mu_o\sin\theta}\, e^{-jk_z z}\, \frac{1}{H_o^{(2)}(k_\varrho a) - j\frac{1}{60\pi\sigma a\sin\theta}H_1^{(2)}(k_\varrho a)} \tag{26}$$

This same result (26) has been obtained from a somewhat different approach and reported by Lee[3]. Thus, it can be seen that the last result is a good approximation for low frequency:

$$\omega << \frac{1}{a^2 \mu_o \sigma}.$$

Frequency response data show that it is actually a good approximation for $0 \leq \omega \leq 10^9$ in most cases of interest.

There is a fundamental difference between the perfect conductor case and the finite conductivity case for very high frequencies (or very early time in the impulse response). It is advantageous to let $s = j\omega$ or $\omega = -js$, so that

$$H_o^{(2)}(\omega a \sin\theta/c) = j\frac{2}{\pi} K_o(sa \sin\theta/c) \rightarrow j \sqrt{\frac{2c}{\pi sa \sin\theta}}\, e^{-sa\sin\theta/c}$$

$$H_1^{(2)}(\omega a \sin\theta/c) = -\frac{2}{\pi} K_1(sa \sin\theta/c) \rightarrow -\sqrt{\frac{2c}{\pi sa \sin\theta}}\, e^{-sa\sin\theta/c}$$

$$J_o(k'_\rho a) \approx I_o(sa \sin\theta/c) \rightarrow \sqrt{\frac{c}{2\pi sa \sin\theta}}\, e^{sa\sin\theta/c}$$

$$J_1(k'_\rho a) \approx -j\, I_1(sa \sin\theta/c) \rightarrow -j \sqrt{\frac{c}{2\pi sa \sin\theta}}\, e^{sa\sin\theta/c}$$

$$\frac{k'_\rho \varepsilon_o}{k_\rho \varepsilon'} \approx 1$$

all for $s \rightarrow \infty$. In this case (1) becomes

$$I_{zc}(s) \rightarrow \frac{4E_o}{\mu_o} \frac{e^{-s(z\cos\theta/c - a\sin\theta/c)}}{\sqrt{\frac{2c\sin\theta}{\pi a}}\, s^{1/2}} \qquad (27)$$

The exponential in (27) contributes the correct time delay such that the wave strikes the wire and the current begins at $t = t' = z\cos\theta/c - a\sin\theta/c$. Ignoring the exponential, the initial value theorem gives $[E_0(s) \equiv 1]$

$$i_{zc}(o) = \lim_{s\to\infty} s\, I_{zc}(s) \to \infty$$

Thus, the impulse response is <u>infinite</u> at $t = t'$ when it begins. Also, for very early time $[E_0(s) \equiv E_0]$

$$i_{zc}(t) \approx \frac{4E_0}{\mu_0}\sqrt{\frac{a}{2c\sin\theta}}\,\frac{1}{\sqrt{t - z\cos\theta/c + a\sin\theta/c}}$$

$$\times\, u(t - z\cos\theta/c + a\sin\theta/c) \qquad (\sigma\to\infty) \tag{29}$$

For the finite conductivity case (24) becomes

$$I_{zc}(s) \to 2E_0\sigma\sqrt{\frac{\pi a c}{a\sin\theta}}\,\frac{e^{-s(z\cos\theta/c - a\sin\theta/c)}}{s^{3/2}} \tag{30}$$

and the initial value theorem gives (ignoring the time delay)

$$i_{zc}(0) = 0 \tag{31}$$

Thus, the impulse response is <u>zero</u> at $t = t'$ when it begins. Also, for very early time $[E_0(s) \equiv E_0]$

$$i_{zc}(t) \approx 4E_0\sigma\sqrt{\frac{\pi a c}{2c\sin\theta}}\,\sqrt{t - z\cos\theta/c + a\sin\theta/c}\; u(t - t')$$

The inequalities governing the early time behavior exhibited by (29) and (32) are

$$\omega >> \frac{c}{a\sin\theta} \text{ and } \omega >> \sigma/\varepsilon_0$$

Except for <u>very</u> small a and (or) $\theta$, the second inequality is <u>dominant</u> and requires $\omega >> 10^{18}$ for the usual conductor. Thus the asymptotic behavior indicated by (29) and (32) is of extremely short range, and is unlikely to have

any effect when the impulse response is convolved with the usual time functions that model the emp.

The case of grazing incidence ($\theta \to 0$) is interesting in that (1) predicts an infinite current induced in a perfectly conducting wire. Equation (24) can be written as

$$I_{zc} = \frac{4 E_o}{\mu_o} \frac{1}{\omega \sin\theta \, H_o^{(2)}(\omega a \sin\theta/c) - f(\theta)} \tag{33}$$

where

$$f(\theta) = \frac{\omega\sqrt{\sin^2\theta + \sigma/j\omega\varepsilon_o}}{1 + \sigma/j\omega\varepsilon_o} H_1^{(2)}(\omega a \sin\theta/c) \frac{J_o(k'_\rho a)}{J_z(k'_\rho a)} \tag{34}$$

The first term in the denominator of (33) goes to zero as $\theta \to 0$ (as in the perfect conductor case), but

$$f(\theta) \to \frac{\omega\sqrt{\sigma/j\omega\varepsilon_o}}{1 + \sigma/j\omega\varepsilon_o} (j2/\pi) \frac{1}{\omega a \sin\theta/c} \frac{J_o(ka\sqrt{\sigma/j\omega\varepsilon})}{J_1(ka\sqrt{\sigma/j\omega\varepsilon_o})}$$

$\theta \to 0$

or $f(\theta) \to \infty$ for $\theta \to 0$. Therefore $I_{zc} \to 0$, and the induced current is zero for $\theta = 0$ when loss is present. This is an expected result.

A mathematical model[4] that has been proposed to represent the emp is

$$E_o(\omega) = E_o \left[ \frac{1}{j\omega + \alpha_1} - \frac{1}{j\omega + \alpha_2} \right] \tag{35}$$

where

$E_o = 52.5 \times 10^3$ volts/meter

$\alpha_1 = 4 \times 10^6$ sec$^{-1}$

$\alpha_2 = 478 \times 10^6$ sec$^{-1}$

## III. RESULTS

Figure 2 is a frequency response graph of $I_{zt}(\omega)$ versus $\omega$ (magnitude and angle) for a typical case: $\theta = 54°$; a = 0.00715 meters; and $\sigma$ = 2.31 x $10^5$, 2.31 x $10^6$, 2.31 x $10^7$ mhos per meter [$E_o(\omega) = 1$]. For $0 \leq \omega \leq 10^7$ the graph indicates a behavior very similar to that for the current in a series RL circuit: the main differences being that the slope is only about -18 dB/decade rather than -20 dB/decade, and the phase begins to slowly increase after approaching -90°. The oscillatory behavior of the Bessel and Hankel functions (that determines the correct delay time and very early time response) has not been reached in Figure 2, but this behavior is not important for $t > 10^{-7}$ seconds, because at $\omega = 10^9$ the magnitude response for the current ($\sigma$ = 2.31 x $10^7$) is down by 126 dB. Furthermore the response of (35) is down by 46 dB. Thus, for the double exponential emp (35) the response is down by about 172 dB at $\omega = 10^9$.

Figure 3 is a frequency response graph of $|I_{zt}/E_o|$ in dB and $\underline{|I_{zt}/E_o}$ in degrees versus $\omega$ (logarithmic scale) for z = 0, a = 0.00715 meters, $\sigma$ = 2.31 x $10^7$ mhos per meter, and $\theta$ = 5°, 18°, 36°, and 90°. Except for very small values of $\theta$, the magnitude response curves break at small values of $\omega$, whereas the poles of the input function are at $\omega$ = 4 x $10^6$ and 478 x $10^6$. This behavior makes it extremely difficult to obtain $i_{zt}(t)$ by numerical inversion of (22). Nevertheless, results are shown in Figure 4 for a = 0.00715, $\sigma$ = 2.31 x $10^7$, and $\theta$ = 18°, 36°, 54°, and 90°. The perfect conductor ($\sigma \to \infty$) case from Barnes[2] is shown for purposes of comparison. As can be seen, the difference is very small, and even if the conductivity is reduced by a factor of 10, the difference is small. The reason for this is obvious in Figure 2. The difference in the

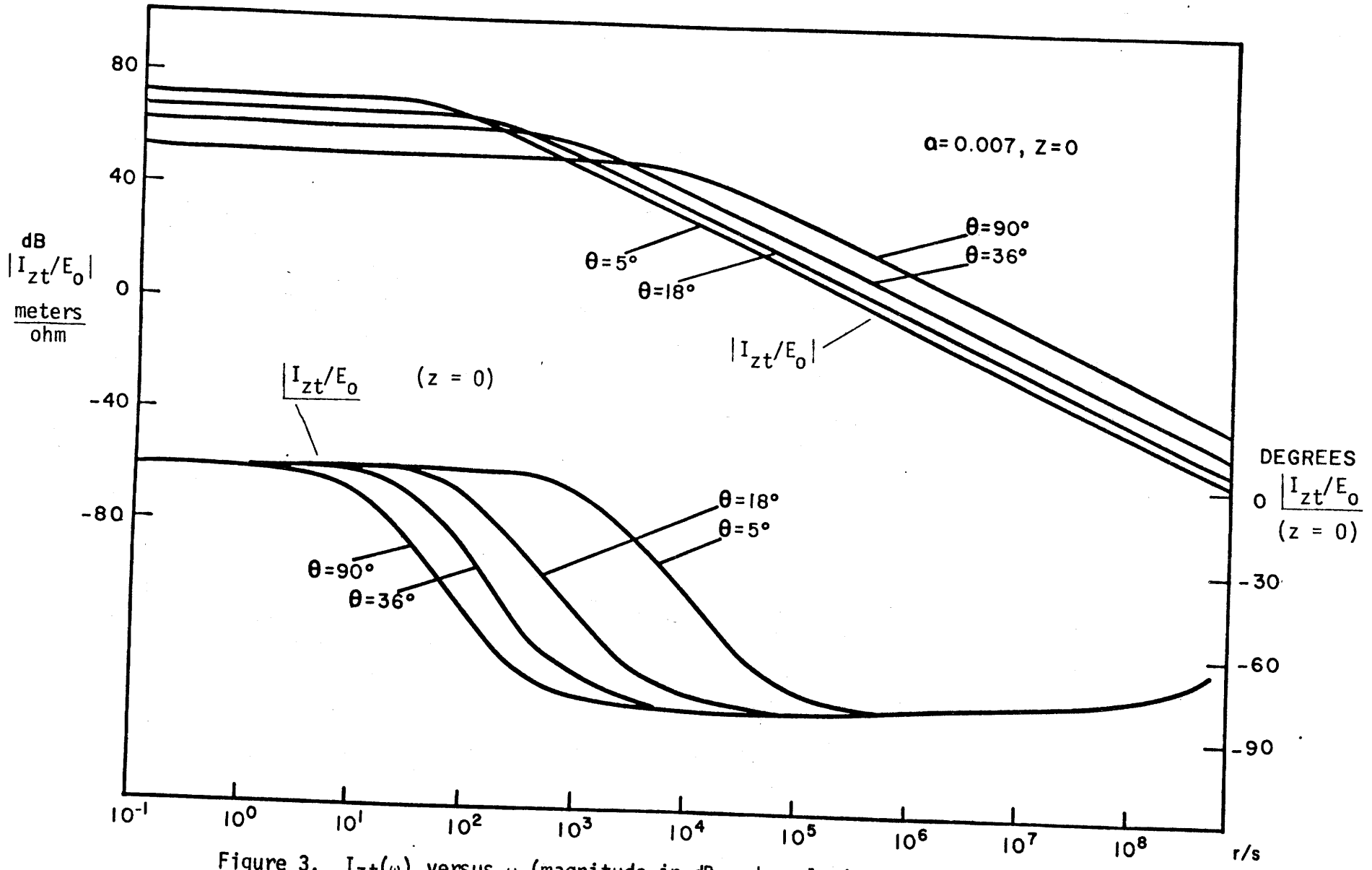


Figure 3. $I_{zt}(\omega)$ versus $\omega$ (magnitude in dB and angle in degrees) for a = 0.00715, $\sigma = 2.31 \times 10^7$, z = 0, $\theta$ = 5°, 18°, 36°, 90°, $E_o = 1$.

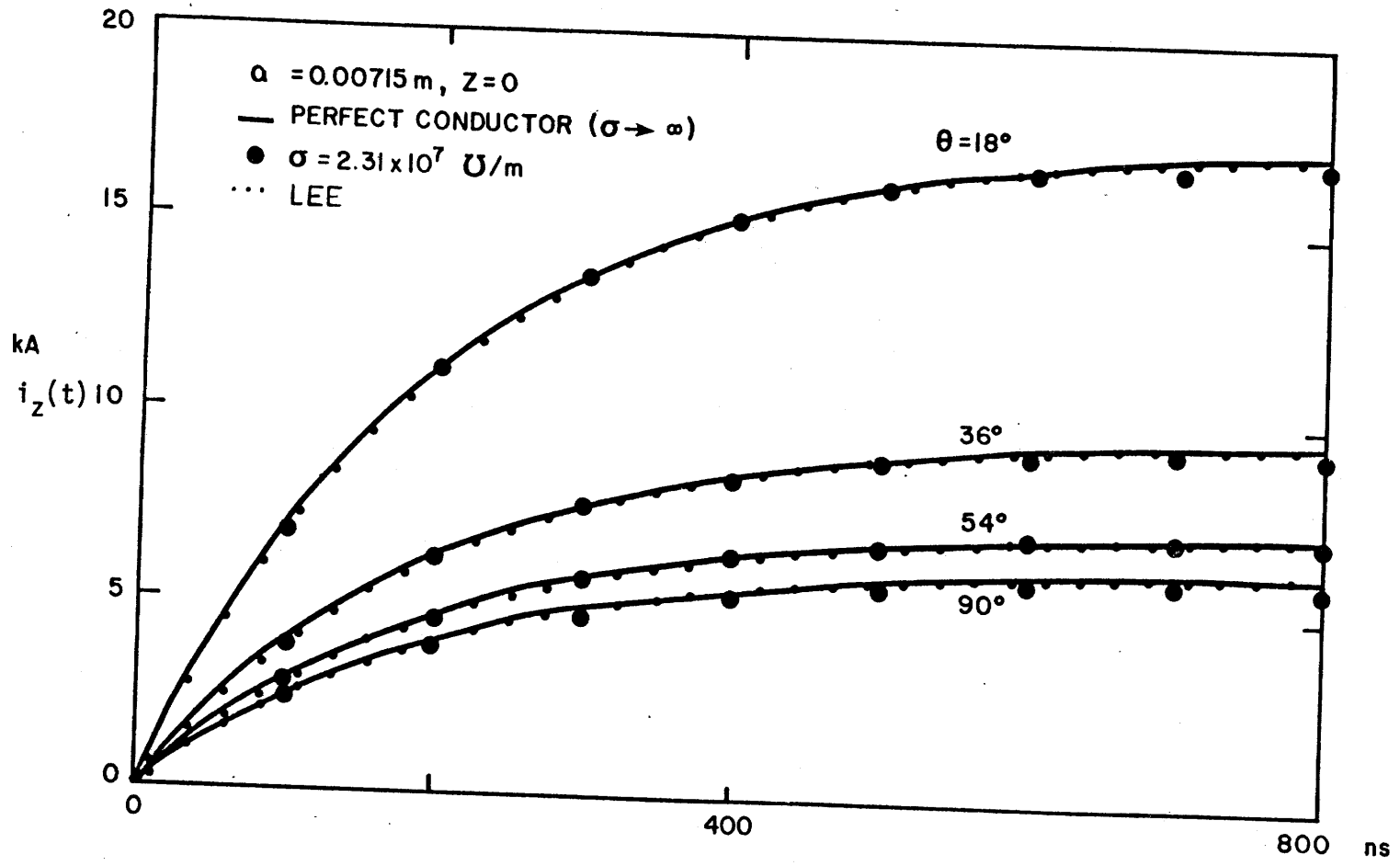


Figure 4. Early-time response due to double exponential EMP; a = 0.00715, $\sigma$ = 2.31 x $10^7$, z = 0, $\theta$ = 18°, 36°, 54°, 90°.

perfect conductor case and the finite conductivity case only occurs at low frequency, and this primarily affects the late time response.

A simple approximation for (22) that can be made for late time is:

$$I_{zt}(\omega) \approx \pi a^2 \sigma \sin\theta \, E_o(\omega) \, b \, \frac{1}{b + (j\omega)^k} \tag{36}$$

Since

$$\frac{t^{k-1}}{\Gamma(k)} - \frac{b}{\Gamma(2k)} t^{2k-1} + \frac{b^2}{\Gamma(3k)} t^{3k-1} - \cdots \longleftrightarrow \frac{1}{b + j\omega^k}$$

$i_{zt}(t)$ can be found by convolution:

$$i_{zt}(t) = \pi a^2 \sigma \sin\theta \, E_o \, b \sum_{n=1}^{\infty} \frac{(-1)^{n+1} (b)^{n-1}}{\Gamma(nk)}$$

$$\bullet \int_0^t x^{nk-1} \left[ e^{-a_1(t-x)} - e^{-a_2(t-x)} \right] dx \tag{37}$$

The simplest way to find appropriate values of k and b is that of choosing a frequency in the middle of the range considered to be important and then forcing the magnitude and phase (separately) of (36) to agree with Figure 2. This gives two equations and two unknowns. For $\sigma = 2.31 \times 10^7$, a = 0.00715, and $\theta = 54°$ (as before) this procedure gives k = 0.9111 and b = 54.77. Results are shown in Figure 5. They agree very well with the perfect conductor case, indicating that (for $\sigma = 2.31 \times 10^7$) the loss is unimportant for early time. For late time this loss is bound to make the current go to zero sooner than with no loss.

Results for a particular late time case using equation (37) are shown in Figure 6. This case is for $\sigma = 2.31 \times 10^7$, a = 0.00715, and $\theta = 54°$. Results are as expected.

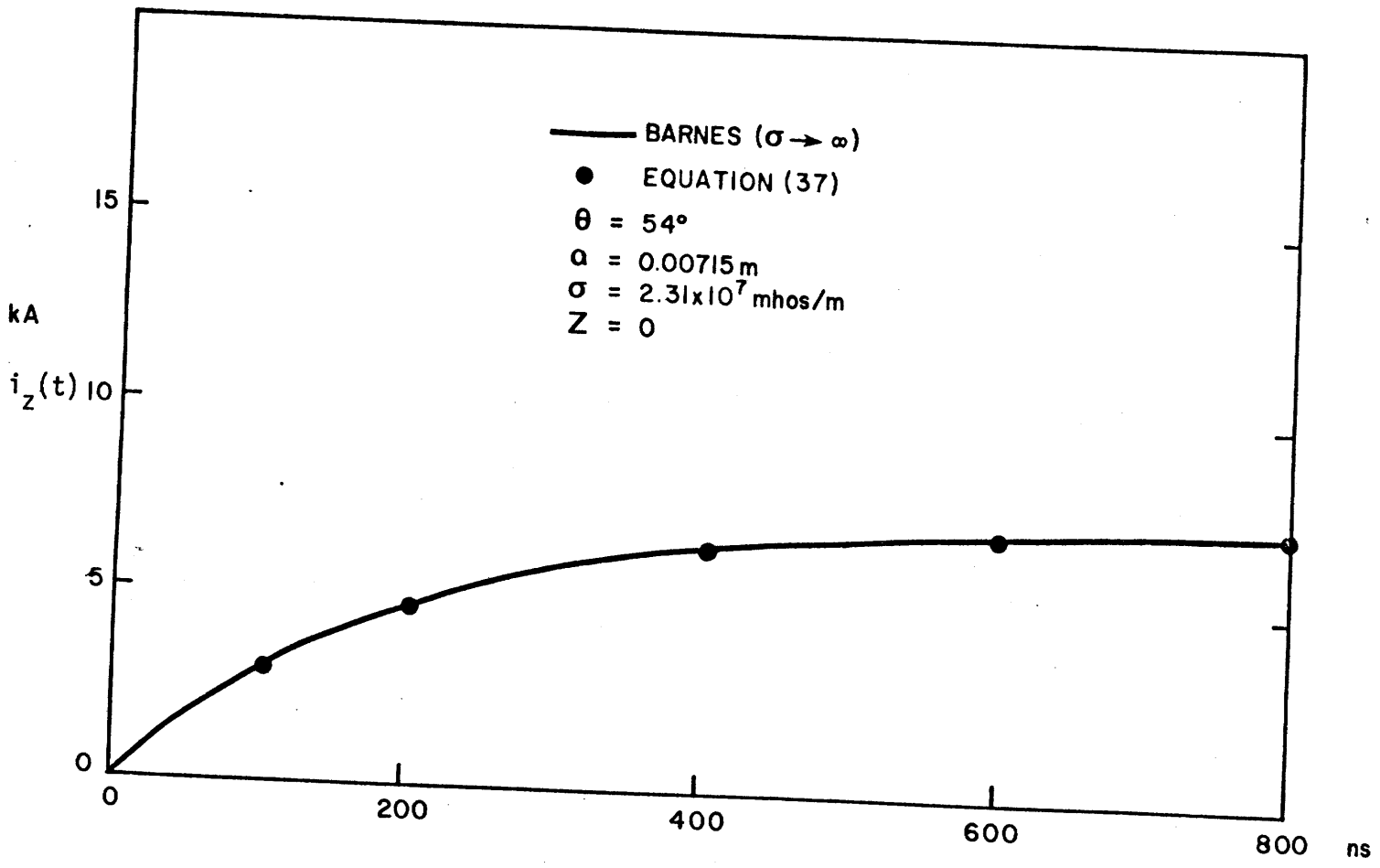


Figure 5. Approximate early-time response (37) due to double exponential EMP; a = 0.00715, $\sigma$ = 2.31 x $10^7$, z = 0, $\theta$ = 54°.

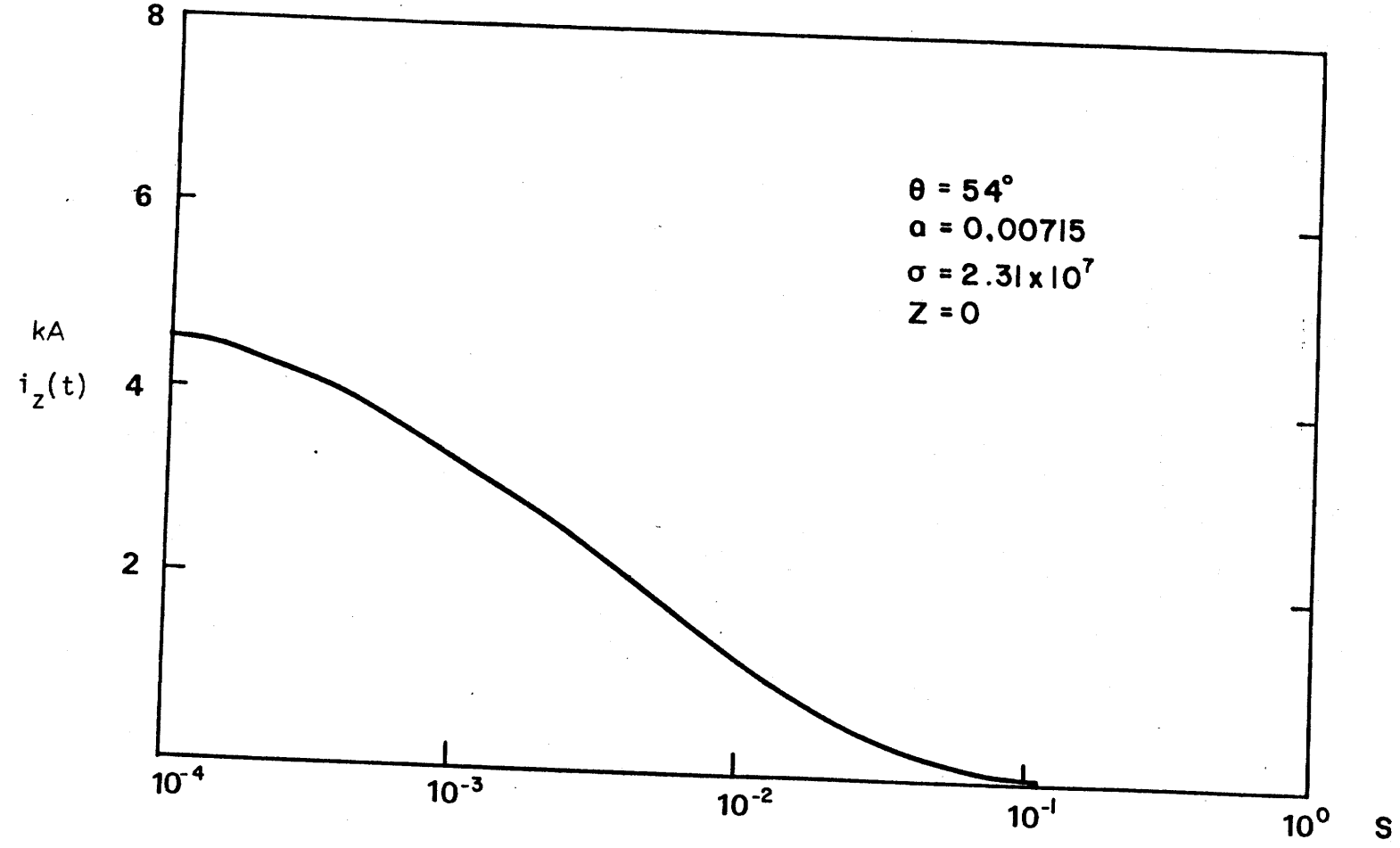


Figure 6. Approximate late-time response due to double exponential EMP; $a = 0.00715$, $\sigma = 2.31 \times 10^7$, $z = 0$, $\theta = 54°$.

Finally, the unit-impulse response for the current has been calculated for a = 0.00715, $\sigma$= 2.31 x $10^7$ and $\infty$, $\theta$ = 90°, 54°, 36°, 18°, and 5°. Notice that $E_0(\omega) \equiv 1$ for the unit-impulse response, and it is measured in ampere-meters per volt-second or meters per ohm-second. The only case for which an appreciably difference occurs is that for $\theta$= 5° (very low angle). Inspection of Figure 3 reveals why this occurs. Remember that the solid curves ($\sigma \rightarrow \infty$) will go to $+\infty$ as t goes to zero, but this behavior is of such short range that it cannot be shown for the time scale used. On the other hand, for $\sigma$= 2.31 x $10^7$ (dotted part), the curves will go to zero as t goes to zero, but this also cannot be shown on Figure 7 for the same reason as given in the preceding sentence.

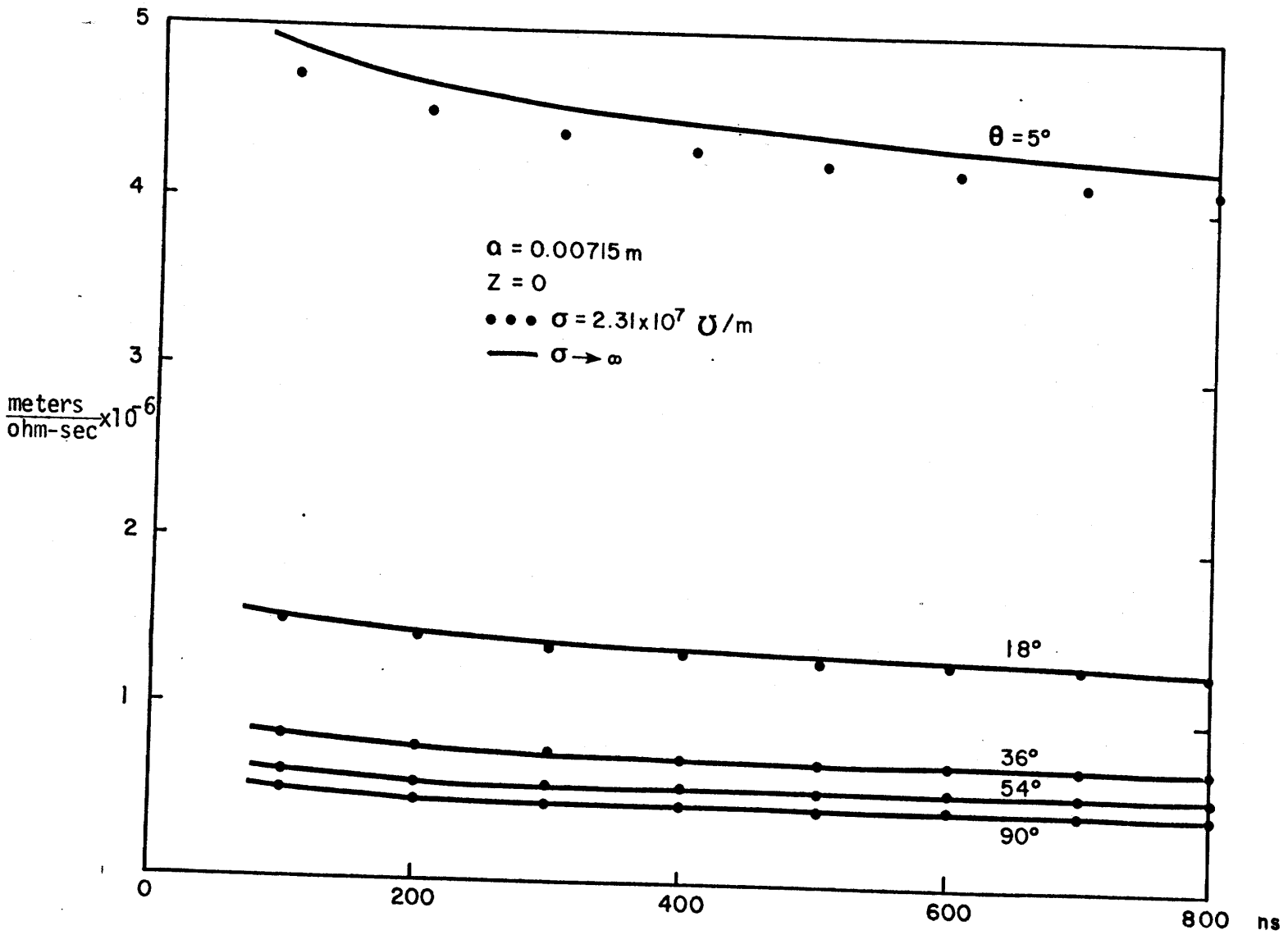


Figure 7. Unit-impulse for the current; a = 0.00715, $\sigma = 2.31 \times 10^7$, z = 0, $\theta$ = 5°, 18°, 36°, 54°, 90°: z = 0, $E_0(\omega) = 1$.

## IV. CONCLUDING REMARKS

For conductor sizes and conductivities like those found in overhead power transmission lines the time-domain induced current differs negligibly from that of the perfect conductor case for $t = 0$ up to about $t = 10^{-4}$s. For $t > 10^{-4}$s the finite conductivity brings the current down sooner than it would come down for $\sigma \to \infty$. This statement is true for all angles ($\theta$) one would normally expect for an emp. If, however, $\theta$ is small, both Figures 3 and 7 indicate that a small difference exists for the induced current between the perfect conductor case and the finite conductivity case. This is an important consideration because when the wire is placed above a finitely conducting ground the incident field plus the field reflected from the ground may be larger than the incident field alone for low angles. This is investigated in a separate work.

## REFERENCES


1. J. H. Marable, H. P. Neff, D. B. Nelson, and J. D. Tillman, "EMP Coupling Studies", Progress Report, ORNL, 1971.
2. P. R. Barnes, "The Axial Current Induced on an Infinitely Long, Perfectly Conducting, Circular Cylinder in Free Space by a Transient Electromagnetic Wave," IN 64, March 1971.
3. K. S. H. Lee, Private Communication.
4. K. S. H. Lee, "EMP Interaction: Principles, Techniques and Reference Data," AFWL, December, 1980.

OAK RIDGE NATIONAL LABORATORY
OPERATED BY MARTIN MARIETTA ENERGY SYSTEMS, INC.

POST OFFICE BOX X
OAK RIDGE, TENNESSEE 37831

July 16, 1985

C. E. Baum
NTYEE
Kirkland AFB, NM 87117

Dear Carl:

All papers and notes submitted to AFWL for publication in the AFWL EMP Note Series are cleared for public release. We have clearance documentation on IN 441, IN 436, and TN 351. The documentation for IN 435 has been misfiled and we are attending to that problem.

Once again, all notes and papers that we submit to your office are cleared. A few notes by LuTech, Inc. will not be submitted to AFWL because of classification. If you have any further questions, please let me know.

Sincerely,

Kindy Barnes

P. R. Barnes

PRB/mm